Environmental Science & Technology

pubs.acs.org/est

Article

Revealing the Marine Cycles of Volatile Sulfur Compounds and Their Biogeochemical Controls: A Case of the Western North Pacific

Feng Xu, Hong-Hai Zhang,* Xiao-Song Zhong, Shi-Bo Yan, Jia-Wei Zhang, Gui-Peng Yang,* Xin Ma, and Zhao-Hui Chen

Cite This: *Environ. Sci. Technol.* 2024, 58, 3235−3245

Read Online

ACCESS | Metrics & More | Article Recommendations | Supporting Information

ABSTRACT: Volatile sulfur compounds, such as dimethyl sulfide (DMS), carbonyl sulfide (OCS), and carbon disulfide (CS_2), have significant implications for both atmospheric chemistry and climate change. Despite the crucial role of oceans in regulating their atmospheric budgets, our comprehension of their cycles in seawater remains insufficient. To address this gap, a field investigation was conducted in the western North Pacific to clarify the sources, sinks, and biogeochemical controls of these gases in two different marine environments, including relatively eutrophic Kuroshio−Oyashio extension (KOE) and oligotrophic North Pacific subtropical gyre. Our findings revealed higher concentrations of these gases in both seawater and the atmosphere in the KOE compared to the subtropical gyre. In the KOE, nutrient-rich upwelling stimulated rapid DMS biological production, while reduced seawater temperatures hindered the removal of OCS and CS_2, leading to their accumulation. Furthermore, we have quantitatively evaluated the relative contribution of each pathway to the source and sink of DMS, OCS, and CS_2 within the mixed layer and identified vertical exchange as a potential sink in most cases, transporting substantial amounts of these gases from the mixed layer to deeper waters. This research advances our understanding of sulfur gas source-sink dynamics in seawater, contributing to the assessment of their marine emissions and atmospheric budgets.

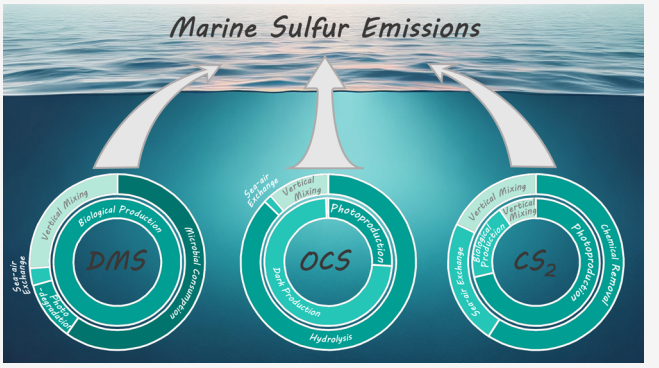

KEYWORDS: *volatile sulfides, DMS, OCS, CS_2, marine sulfur emissions, Pacific Ocean*

1. INTRODUCTION

Volatile sulfur compounds, such as dimethyl sulfide (DMS), carbonyl sulfide (OCS), and carbon disulfide (CS_2), play an important role in both atmospheric chemistry and climate change.[1−3] The oxidation products of atmospheric DMS, such as methanesulfonic acid and sulfate, are the dominant contributors to cloud condensation nuclei in the marine boundary layer,[4−6] which can influence the radiation budget and climate feedback. However, the exact role that DMS plays in regulating our climate is still a matter of debate.[7,8] OCS is the most abundant sulfur-containing trace gas in the atmosphere and is also climate-relevant because it can change the energy budget as a greenhouse gas in the troposphere.[3] Besides, due to its long tropospheric lifetime of 2−7 years,[9] OCS can be transported to the stratosphere, where it is considered a major precursor of sulfate aerosols.[10] CS_2 in the atmosphere indirectly affects climate as an important precursor of OCS.[3,11]

The global ocean plays a crucial role in regulating the atmospheric budgets of DMS, OCS, and CS_2.[9,12,13] Marine DMS is primarily derived from the enzymatic breakdown of dimethyl sulfoniopropionate (DMSP), generally found in phytoplankton cells. It is estimated that approximately 27.1 Tg of sulfur, in the form of DMS, is emitted from the ocean annually.[12] Besides, sea surface DMS can be removed through microbial metabolism and photo-oxidation.[14,15] OCS is generally produced via reactions between ultraviolet radiation and dissolved organic sulfur,[16−18] which is an indirect process photosensitized by chromophoric dissolved organic matter (CDOM). The reaction of sulfur radicals[19] can also produce OCS in the dark. Hydrolysis and outgassing to the atmosphere are the known removal pathways for marine OCS. Marine emissions contribute significantly to the global OCS budget, as OCS can enter the atmosphere directly via oceanic emissions and indirectly via the oxidation of atmospheric DMS and CS_2.[3,20] Production and loss processes for marine CS_2 are less well-constrained. Similar to the OCS, CS_2 in seawater may originate from photoreactions of organic sulfur. Evidence for biological production comes from laboratory culture experiments;[21] however, verification in situ is lacking. Hydrolysis,

Received: September 12, 2023
Revised: January 22, 2024
Accepted: January 24, 2024
Published: February 12, 2024

https://doi.org/10.1021/acs.est.3c07498
Environ. Sci. Technol. 2024, 58, 3235−3245

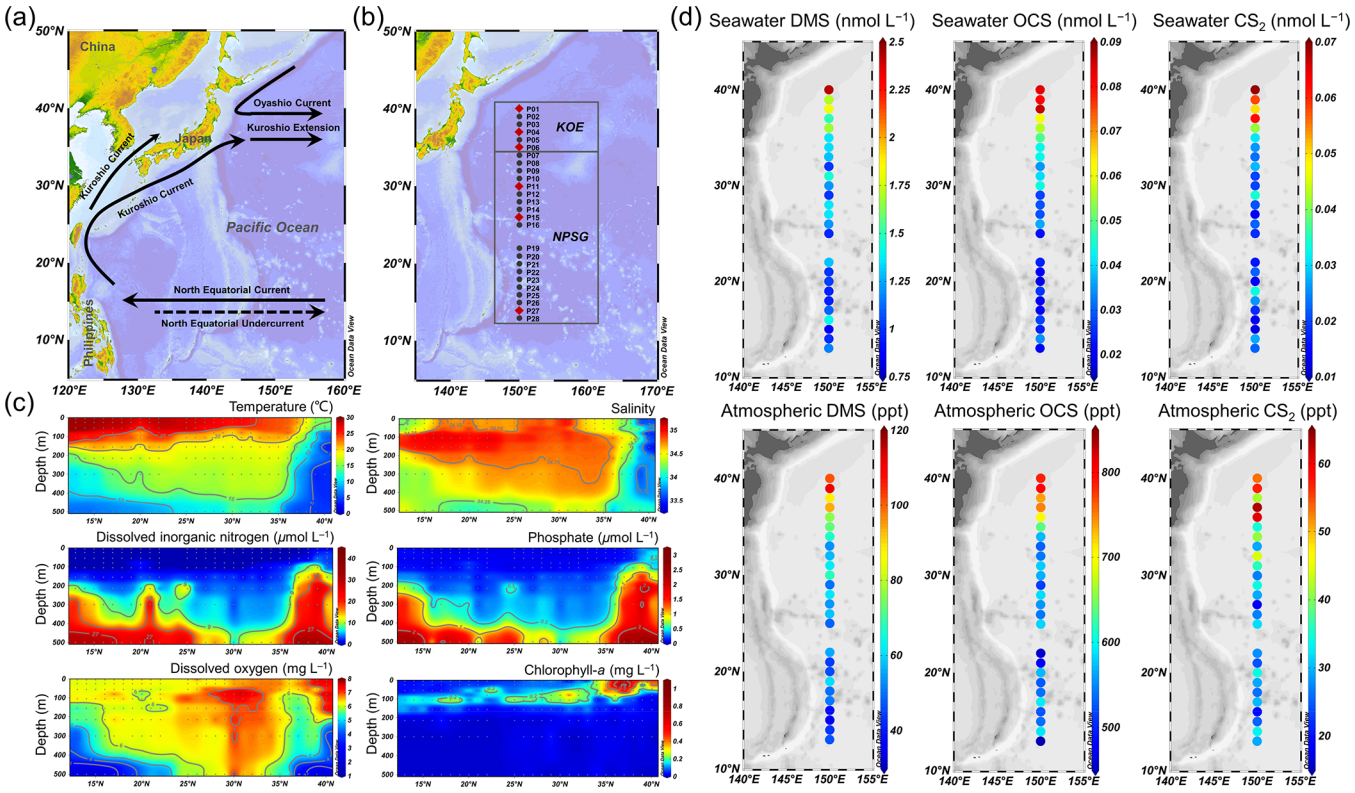

Figure 1. (a) Major ocean currents in the western North Pacific. (b) Locations of sampling stations (red diamond represents the station for incubation and irradiation experiments). (c) Vertical profiles (0−500 m) of temperature, salinity, dissolved inorganic nitrogen, phosphate, dissolved oxygen, and chlorophyll-*a* in the 150°E section. (d) Horizontal distribution of DMS, OCS, and CS_2 in the surface seawater (about 5 m) and overlying atmosphere.

oxidation, and outgassing to the atmosphere are currently known sinks of marine CS_2;[22] however, more chemical pathways need to be explored to explain observed CS_2 concentrations.[23] Marine emission is the second most important source of atmospheric CS_2 after industrial emission.[3]

The significant role that the ocean plays in the emission of DMS, OCS, and CS_2 necessitates the exploration of their biogeochemical cycles in seawater. The western North Pacific is a typical marine environment with many different types of marine ecosystems and currents, playing an important role in global sea-air exchange.[24] The convergence of the southward-flowing cold Oyashio Current with the northward-flowing warm Kuroshio Current in the region east of Japan results in one of the most energetic regions in the global ocean, namely, Kuroshio-Oyashio extension (KOE) where prominent mesoscale dynamics persistently occur, such as fronts and eddies.[25,26] The abundance of nutrients from eddy-induced upwelling increases primary productivity and changes the biochemical environment of the upper ocean in the KOE.[27] In contrast, the North Pacific subtropical gyre (NPSG) is regarded as one of the world's largest ocean deserts due to its persistent nutrient depletion and low organism standing stocks. The KOE region has been identified by previous research[9,14,28] as a hotspot for DMS, OCS, and CS_2. However, the deep exploration of the underlying biogeochemical mechanisms, particularly those governing OCS and CS_2, under varying oceanographic conditions is significantly insufficient. New evidence suggests an elevated vegetation sink for OCS, which leads to a discrepancy in its tropospheric budget, with most studies suggesting that oceanic emissions might account for this gap.[29,30] Nonetheless, inadequate OCS and CS_2 cycle studies generate vast uncertainty in the estimated oceanic sources of OCS and its precursor CS_2,[13,31] making it even harder to balance the atmospheric OCS budget.

To bridge existing knowledge gaps, we quantified the concentrations of DMS, OCS, and CS_2 in the seawater and the atmosphere of the western North Pacific. We also examined the primary production and loss processes of marine DMS, OCS, and CS_2. Using this information, we determined the source-sink budgets for these gases within the mixed layer and evaluated the relative contribution of each pathway to the overall source-sink dynamics quantitatively. Consequently, we identified the biogeochemical mechanisms behind the production, removal, and emission of DMS, OCS, and CS_2 in different marine environments. Our research constrained the cycle of sulfur gases in seawater, diminishing uncertainties in marine emissions. This facilitates enhanced assessments of their atmospheric budgets and climate impacts in future modeling studies.

2. METHODS

2.1. Sampling and Analysis. Our investigation was carried out on the research vessel "*Dong Fang Hong* 3" in the western North Pacific in November 2019, as shown in Figure 1a. Seawater samples were collected from all 26 stations (Figure 1b) using 12-L Niskin bottles equipped with a Seabird 911 conductivity−temperature-depth sensor rosette, which facilitated the simultaneous measurement of the seawater temperature and salinity. The samples were subsequently analyzed for several parameters, e.g., DMSP, DMS, OCS, CS_2, nutrients, chlorophyll-*a*, phytoplankton abundance, and DMSP lyase activity. Moreover, air samples were collected for the measurement of atmospheric DMS, OCS, and CS_2 from each station.

https://doi.org/10.1021/acs.est.3c07498
Environ. Sci. Technol. 2024, 58, 3235−3245

The sea-air fluxes of DMS, OCS, and CS_2 were calculated by the W2014 method.[32] Detailed methods for sampling, measurement, and calculation as well as statistics and uncertainty analysis are provided in Appendixes S1 and S2. In addition, incubation and irradiation experiments were conducted at six selected stations.

2.2. Determination of Production and Loss Rates of Marine DMS, OCS, and CS_2. *2.2.1. Dark Incubations.* The rates of DMS biological production, microbial consumption, and dissolved DMSP degradation in surface seawater were measured using competitive inhibition assays.[33,34] Dimethyl disulfide[33] and glycine betaine[34] served as the consumption inhibitors for DMS and dissolved DMSP, respectively. Specifically, blank, dimethyl disulfide-added (260 μmol L^{-1}), and glycine betaine-added (5 μmol L^{-1}) seawater samples were incubated for 6 h at in situ seawater temperatures in 500 mL airtight glass syringes in darkness. Subsamples. were collected at 0, 3, and 6 h in triplicate for DMS and dissolved DMSP analysis. The gross and net biological production rates of DMS were inferred from the slope of DMS concentration over time in inhibitor-added and blank groups, respectively, with the difference indicating the microbial consumption rate of DMS. A similar approach was used to calculate the dissolved DMSP degradation rate. The *net-loss curve* approach suggested the absence of DMSP synthesis in the dark and a first-order reaction for total DMSP loss rate.[35] Hence, we also measured the total DMSP concentration in the blank sample at 0, 3, and 6 h, with the loss rate constant equating to the slope of the natural logarithm of total DMSP concentration over time. The fitting results are shown in Figure S1.

As for OCS and CS_2, both filtered (via 0.45 and 0.22 μm polyethersulfone ultrafiltration membranes sequentially to eliminate biological influences) and unfiltered seawater were incubated airtightly at in situ seawater temperatures for 12 h in the dark at these stations. During incubation, subsamples were collected at 0, 6, and 12 h to determine the OCS (unfiltered group) or CS_2 concentration (both groups). Regarding CS_2, we can safely assume that biological production does not occur within the filtered seawater. As such, the slope of CS_2 concentration versus time in the filtered group can represent the chemical removal rate of CS_2, such as hydrolysis and oxidation.[22] In contrast, unfiltered seawater encompassed both the chemical removal and biological production of CS_2. Thus, the biological production rate of CS_2 was deduced by contrasting the slopes of CS_2 concentration against time between unfiltered and filtered groups. However, dark production and hydrolysis processes of OCS are present in both filtered and unfiltered seawater. Therefore, the first step was determining the OCS hydrolysis rate ($R_{hydrolysis}$, nmol L^{-1} s^{-1}) using the following empirical formula:[36,37]

$$R_{hydrolysis} = [OCS] \times [\exp(24.3 - \frac{10,459}{T}) + \exp(22.8 - \frac{6040}{T}) \times \frac{K_w}{a(H^+)}]$$

$$-\log_{10} K_w = \frac{3046.7}{T} + 3.7685 + 0.0035486 \times S^{0.5}$$

where [OCS], T, and S represent the seawater OCS concentration (nmol L^{-1}), temperature (K), and salinity, respectively. The $a(H^+)$ was the proton activity, which was equivalent to 10^{-pH}. Considering the high measurement precision of temperature, salinity, and pH (see Appendix S1 for details), the uncertainty in the calculated rate was mainly derived from the OCS measurement, resulting in an approximate uncertainty of 3%. The dark production rate of OCS was calculated as the change rate in the unfiltered group (slope of concentration versus time) plus the calculated hydrolysis rate.

2.2.2. Irradiation Experiments. The rates of DMS photodegradation, as well as the rates of OCS and CS_2 photoproduction, were also measured. To minimize biological and particulate interference, surface seawater was sequentially filtered through 0.45 and 0.22 μm polyethersulfone ultrafiltration membranes using low-vacuum suction. The filtered seawater was then placed in quartz tubes for exposure to different light conditions: full-spectrum solar radiation (no treatment), photosynthetically active radiation (PAR; one layer of UF3 Plexiglas), PAR and ultraviolet A radiation (UVA; one layer of Mylar-D), and darkness (three layers of aluminum foil). The dark group was implemented to adjust concentration shifts caused by possible dark processes. Quartz tubes were immersed in a shallow water bath incubator to maintain in situ temperatures and expose them to ambient solar radiation. Incident photon flux density was regularly monitored using a calibrated portable high-accuracy UV−visible spectroradiometer (OL 756, Gooch & Housego, UK). Subsamples were collected at 0, 3, 6, and 9 h to determine the concentrations of DMS, OCS, and CS_2. The rate constant (k_t, h^{-1}) of DMS photodegradation at the sea surface was calculated based on the pseudo-first-order kinetics equations:

$$-d[DMS]/dt = k_t \times [DMS]$$

$$k_t = -\ln([DMS]_t/[DMS]_0)/t$$

Similarly, the rate constants (k_{photon}, m^2 E^{-1}) normalized by photon flux were calculated:

$$-d[DMS]/dt = k_{photon} \times [DMS] \times PFD$$

$$k_{photon} = -\ln([DMS]_t/[DMS]_0)/J$$

where $[DMS]_t$ and $[DMS]_0$ represent DMS concentration (nmol L^{-1}) at time t and time 0, respectively; PFD and J are the instantaneous (E m^{-2} h^{-1}) and cumulative photon flux density (E m^{-2}), respectively. The photoproduction rates of OCS and CS_2 with respect to time (R_t, nmol L^{-1} h^{-1}) and photon flux (R_{photon}, nmol L^{-1} m^2 E^{-1}) at the sea surface were calculated based on the following formula:

$$R_t = \Delta[OCS/CS_2]/\Delta t$$

$$R_{photon} = \Delta[OCS/CS_2]/\Delta J$$

Consequently, the DMS photodegradation rate constant and the photoproduction rates of OCS and CS_2 were calculated based on the slopes of the natural logarithm of DMS concentration over time and the slopes of OCS/CS_2 concentration over time, respectively. The ultraviolet B (UVB) radiation results were attained by deducting the UVB-filtered light observations from those of full-spectrum solar radiation. Considering the average daylight duration of approximately 13 h, the hourly rates (expressed in nmol L^{-1} h^{-1}) were converted to daily rates (nmol L^{-1} d^{-1}) by multiplying them by 13. The photoreaction rates in the water column should be adjusted using the following formula:

$$k_t(X, Z) = k_t(X, 0) \times PFD(X, Z)/PFD(X, 0)$$

https://doi.org/10.1021/acs.est.3c07498
Environ. Sci. Technol. 2024, 58, 3235−3245

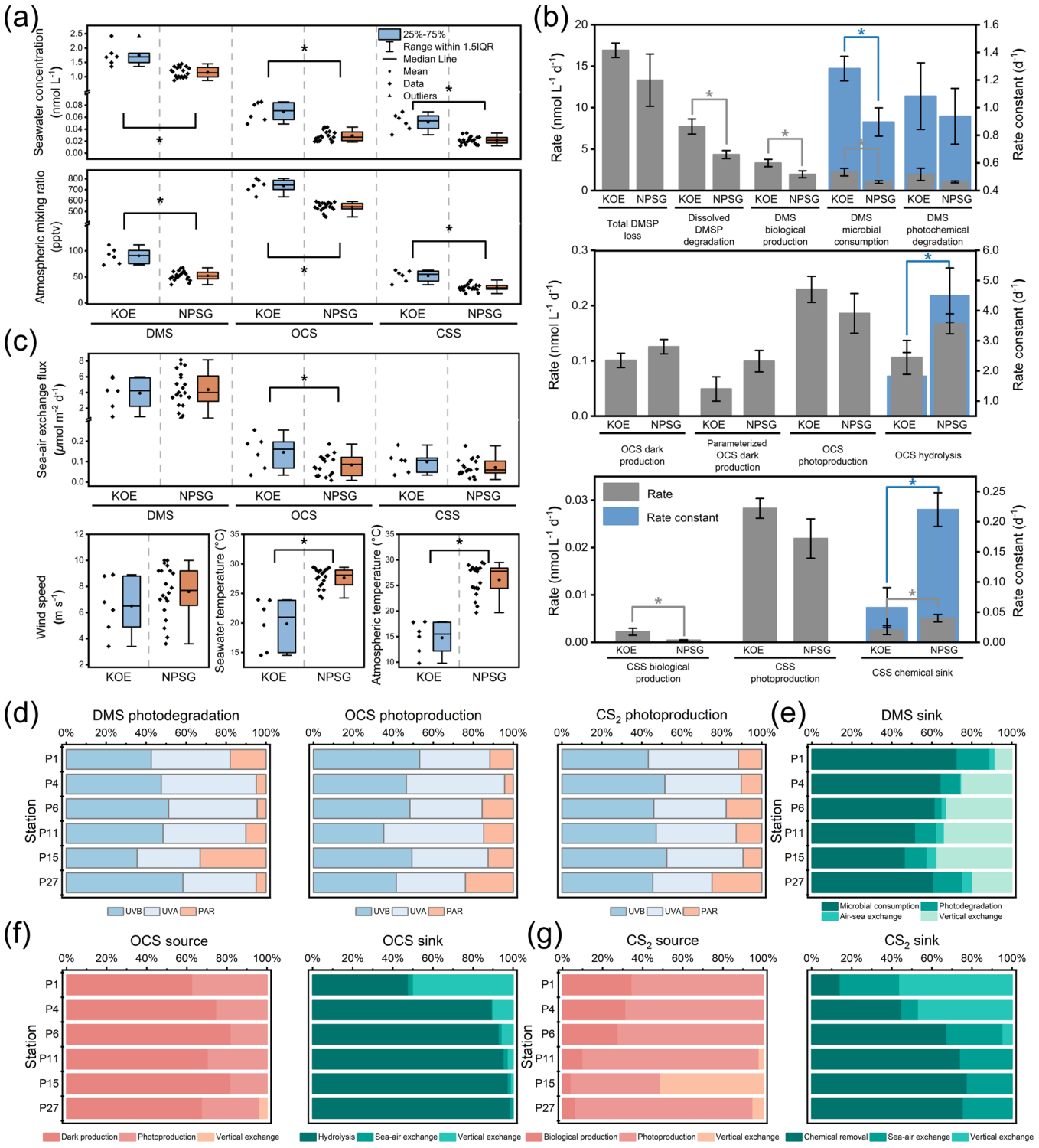

Figure 2. (a) Boxplot of DMS, OCS, and CS_2 concentrations in the surface seawater and overlying atmosphere (the number of sampling stations in the KOE and NPSG is 6 vs 20). (b) Bar chart of primary source and sink rates of marine DMS, OCS, and CS_2 (the error bars represent the standard deviation; 3 vs 3). (c) Boxplot of sea-air exchange fluxes, wind speed, seawater temperature, and atmospheric temperature (6 vs 20). Asterisks represent significant differences between the two sets of data (t test, $P < 0.05$). (d) Relative contribution of each radiation to the photodegradation of DMS, as well as to the photoproduction of OCS and CS_2 in the surface seawater. Relative contribution of each process to (e) DMS removal and (f) OCS and (g) CS_2 source and removal in the mixed layer.

$$R_t(X, Z) = R_t(X, 0) \times \mathrm{PFD}(X, Z)/\mathrm{PFD}(X, 0)$$

where $k_t(X,Z)$ and $R_t(X,Z)$ represent the rate constant and rate under the X radiation at Z of depth ($\mathrm{PFD}(X,Z)$), respectively. Since we only measured the light intensity on the sea surface, the light intensity for X type of radiation at Z depth ($\mathrm{PFD}[X,Z]$) was calculated from the light intensity at the surface ($\mathrm{PFD}[X,0]$) by exponentially decreasing it with depth according to the Beer–Lambert equation:

https://doi.org/10.1021/acs.est.3c07498
Environ. Sci. Technol. 2024, 58, 3235−3245

$$\mathrm{PFD}(X, Z) = \mathrm{PFD}(X, 0) \times e^{-k_X Z}$$

The light attenuation coefficients at the Napierian logarithm scale (k_X, m^{-1}) for UVB and UVA were approximated as the absorption coefficient of water plus that of CDOM at the corresponding wavelength ($a_W(X)$ and $a_{CDOM}(X)$, m^{-1}) using the following equations:

$$k_{UVB} = a_W(UVB) + a_{CDOM}(UVB)$$

$$k_{UVA} = a_W(UVA) + a_{CDOM}(UVA)$$

Phytoplankton has been shown to attenuate PAR, and its attenuation coefficient (k_{PHY}, m^{-1}) can be assumed to be linearly correlated to chlorophyll-*a* concentration ([CHL], mg L^{-1}):[38]

$$k_{PHY} = 0.03 \times [CHL]$$

Hence, the light attenuation coefficient for PAR (k_{PAR}, m^{-1}) was calculated as follows:

$$k_{PAR} = a_W(PAR) + a_{CDOM}(PAR) + k_{PHY}$$

Note that the described equations are applicable solely within the mixed layer, characterized by uniform properties. The mixed layer depth (MLD) was determined based on the density criterion of 0.03 kg m^{-3} (to the reference depth of 10 dbar), as recommended by de Boyer Montégut et al.[39] By vertically integrating the photoreaction rate of *X* type of radiation across the entire mixed layer and subsequently dividing it by the corresponding MLD (m), we arrived at an average photoreaction rate of *X* type of radiation for the mixed layer ($A_{PR}(X)$, nmol L^{-1} d^{-1}):

$$A_{PR}(X) = \left[\int_0^{MLD} R_t(X, Z) \times dZ\right]/MLD$$

3. RESULTS AND DISCUSSION

3.1. Background of the Western North Pacific. Vertical profiles of temperature, salinity, nutrients, dissolved oxygen, and chlorophyll-*a* at a depth of 0−500 m in the western North Pacific are presented in Figure 1c. The hydrologic characteristics of the survey area are described in detail in Appendix S3. Based on the geographical location, ocean currents, and environmental characteristics, the survey area was classified into two provinces: KOE and NPSG. The means (ranges) of concentrations of DMS, OCS, and CS_2 were 1.29 ± 0.34, 0.038 ± 0.020, and 0.029 ± 0.015 nmol L^{-1} in surface seawater (about 5 m) and were 61 ± 19, 586 ± 93, and 35 ± 12 ppt (volume ratio) in the marine atmosphere, respectively (see Table S1 for details). Our results were consistent with previous studies conducted in the Pacific Ocean.[9,14,37] Both seawater and atmospheric concentrations of DMS, OCS, and CS_2 exhibited a declining trend from north to south (Figure 1d), and all concentrations showed significant differences between the two regions (Figure 2a). To explore the biogeochemical processes governing DMS, OCS, and CS_2, the primary production and loss processes of marine DMS, OCS, and CS_2 have been examined and will be discussed in the following sections (see Tables S2−S6 for details).

3.2. Production Processes of DMS, OCS, and CS_2. *3.2.1. DMSP Loss and DMS Production.* Average rates of total DMSP loss, dissolved DMSP degradation, and DMS biological production in the surface seawater were 15.11 ± 2.93, 6.03 ± 1.84, and 2.64 ± 0.80 nmol L^{-1} d^{-1}, respectively. Notably, elevated rates of dissolved DMSP degradation and DMS biological production were observed in the KOE (Figure 2b). Enhanced surface primary productivity in the KOE, as evidenced by chlorophyll-*a* (Figure 1c) and phytoplankton (Figure S2), was likely attributable to nutrient-rich upwellings (Figure 1c). Higher primary productivity elevated the level of DMS precursor, biogenic DMSP (Figure S3), which can be enzymatically cleaved by heterotrophic bacteria and certain phytoplankton species to produce DMS.[40] Additionally, stronger DMSP lyase activity was observed in KOE seawater (Table S2). In our study, the DMSP concentration and DMSP lyase activity (Figure S4) can explain most of the variations of dissolved DMSP degradation rate (R^2: 79.6% and 77.9%) and DMS biological production rate (84.7% and 71.0%). Consequently, the abundance of DMSP and robust DMSP lyase activity in the KOE were likely key drivers of accelerated DMSP degradation and DMS production. These closely linked processes also led to significant positive correlations between chlorophyll-*a*, DMSP, and DMS concentrations in seawater, with chlorophyll-*a* and DMSP accounting for 47.1% and 72.2% of DMS concentration variability, respectively.

The DMS yield,[41,42] referring to the ratio of DMS biological production rate to total DMSP loss rate, was utilized to estimate the proportion of DMSP converted into DMS. A DMS yield of 17.2% ± 2.6%, significantly lower than the previous study conducted in continental seas (38% ± 9%),[15] indicated that most DMSP did not undergo cleavage to DMS. Instead, demethylation of DMSP into methanethiol happened more easily as it is less energy-intensive for bacteria to form proteins using methanethiol than DMS,[43] particularly in the oligotrophic western North Pacific. Similarly, the relatively high DMS yield was observed in the relatively fertile KOE (19.5% ± 1.6%) than in the oligotrophic NPSG (14.8% ± 0.4%). As Figure S4 indicates, the nutrient-abundant environment of the KOE not only fostered DMSP degradation but also slightly enhanced the DMSP cleavage pathway, collectively boosting the biological production of DMS.

3.2.2. Dark Production of OCS and Biological Production of CS_2. The mean rates of OCS dark production and CS_2 biological production were 0.113 ± 0.018 and 1.34 × 10^{-3} ± 1.04 × 10^{-3} nmol L^{-1} d^{-1}, respectively, as detailed in Tables S3 and S4. The OCS dark production rate was comparable to that in the Sargasso Sea (7.4 ± 1.8 pmol L^{-1} h^{-1}),[44] while reports on CS_2 biological production rates in seawater are scarce. Two mechanisms currently exist for OCS dark production: an abiotic reaction involving sulfur radicals formed by oxygen or metal complexes[19] and a coupling to microbial processes during organic matter remineralization.[45] Therefore, abundant organic matter (Figure S3) and high primary productivity in the KOE theoretically can promote OCS dark generation. However, the dark production rates of OCS in the KOE and the NPSG did not significantly differ (Figure 2b). Intriguingly, higher concentrations of organic matter, as indicated by the CDOM absorption coefficient at 350 nm, correlated with lower OCS dark production rates (Figure S4). We believe that the lower seawater temperature in the KOE may have inhibited the dark production of OCS.[46,47] A significant positive correlation between OCS production rate and seawater temperature underscored the substantial influence of temperature variations on OCS dark production, potentially overshadowing the role of organic matter.

Von Hobe et al.[47] first proposed the parametrization of OCS dark production as a function of seawater temperature (*T*, K) and CDOM absorption coefficient at 350 nm (a_{350}, m^{-1}). To verify the accuracy of the parametrized results, we calculated the

https://doi.org/10.1021/acs.est.3c07498
Environ. Sci. Technol. 2024, 58, 3235−3245

dark production rate (R_{dark}, nmol L^{-1} s^{-1}) based on the recently updated formula,[37] as follows:

$$R_{dark} = a_{350} \times \exp(57.2 - 16200/T) \times 10^{-6}$$

Overall, the calculated rates (Table S3) demonstrated an increasing trend from the north to south similar to our measured rates. However, these calculated rates were consistently lower than the in situ measurements, with the discrepancy widening at lower temperatures. Notably, at Station P2, characterized by the lowest seawater temperature, the measured rate was over four times higher than the calculated rate. This suggests that while seawater temperature significantly influences OCS dark production, its representation in the empirical formula may be excessively weighted, particularly at lower temperatures. The formula can generally be used to forecast dark production of OCS on a large scale, but it might underestimate the OCS production, especially at high latitudes.

CS_2 biological production rates were significantly higher in the KOE compared to the NPSG, with a 10-fold variation (Table S4), primarily due to the elevated phytoplankton abundance. Evidence for algal production comes from laboratory cultures,[21] indicating varying CS_2 production for different phytoplankton species. Interestingly, we found that the CS_2 biological production rate at station P4 with the highest phytoplankton abundance (~96,800 cell L^{-1}) was lower than that at station P1 with a relatively low phytoplankton abundance (~7800 cell L^{-1}). Considering the phytoplankton community structure, specifically the markedly higher abundance of dinoflagellates at P1 (~1500 cells L^{-1}) compared to P4 (~800 cells L^{-1}), we guess that dinoflagellates may have a relatively stronger CS_2 production capacity than diatoms. Furthermore, chlorophyll-*a* concentration can account for 80.6% of the variation in CS_2 biological production rate in the surveyed area (Figure S4), indicating the potential for using remote sensing retrieval of chlorophyll-*a* concentration to predict the CS_2 biological production rate in future studies.

3.2.3. Photoproduction of OCS and CS_2. The rates of photoproduction for OCS and CS_2 at the sea surface, indicating the rapidity of photoreactions under unattenuated in situ solar radiation, were significantly higher than their respective dark and biological production rates, averaging 0.208 ± 0.037 and 2.51 × 10^{-2} ± 4.58 × 10^{-3} nmol L^{-1} d^{-1}. The OCS rate aligned with previous findings in the Sargasso Sea (0.2 nmol L^{-1} d^{-1}).[44] While CS_2 in situ photoproduction has not been reported, both the experimentally derived apparent quantum yield[48] and model simulation[16] indicated its rate is significantly lower than that of OCS, by 5 to 70 times, which our findings confirmed. The photoproduction of OCS and CS_2 is primarily a secondary photoreaction mediated by photosensitizers.[19] After normalizing by photon flux density, OCS and CS_2 photoproduction rates in the KOE significantly exceeded those in the NPSG (Table S5), which indicated abundant photosensitizers and/or precursors in the KOE. Figures S3 and 1c demonstrated that KOE upwelling likely influenced the availability of dissolved organic matter and nitrate for solar radiation exposure, enriching surface photochemical processes with photosensitizers and precursors.[16,49] Additionally, upwelling-associated nutrient influx boosted surface phytoplankton growth, furthering in situ organic matter production. Lennartz et al. also suggested upwelling regions as potential hotspots for OCS and CS_2 photoproduction.[16] Despite the NPSG's lower abundance of photosensitizers and precursors compared to the KOE, its lower latitude resulted in stronger solar radiation, accelerating photochemical processes. At Station P27, with the strongest solar radiation, the unnormalized rates of the photoproduction of OCS and CS_2 rivaled those in the KOE.

The effects of different radiation wavebands on the photoproduction of OCS and CS_2 were explored. The photoproduction rates driven by UVB, UVA, and PAR at the sea surface (Tables S3 and S4) were 0.096 ± 0.025, 0.083 ± 0.015, and 0.029 ± 0.014 nmol L^{-1} d^{-1} for OCS and were 1.19 × 10^{-2} ± 2.25 × 10^{-3}, 9.48 × 10^{-3} ± 2.10 × 10^{-3}, and 3.69 × 10^{-3} ± 1.65 × 10^{-3} nmol L^{-1} d^{-1} for CS_2. As shown in Figure 2d, the relative contributions of UVB, UVA, and PAR to total photoproduction were 45.6% ± 5.8%, 40.5% ± 6.5%, and 13.8% ± 5.8% for OCS, and 47.6% ± 3.3%, 37.9% ± 4.6%, and 14.5% ± 5.4% for CS_2. More than 80% of photoproduction of both the OCS and CS_2 was driven by UV radiation. Similar wavelength dependence of OCS photoproduction was also reported by Li et al. through laboratory culture.[49] This phenomenon may be due to the photosensitizers having wavelength-selective absorption and mainly absorbing UV radiation. For example, CDOM dissolved in seawater is easily excited by UV radiation and forms an excited-state CDOM (^{3}CDOM*) to participate in the formation of COS and CS_2. The rates under UVB, UVA, and PAR at the sea surface were normalized by corresponding photon flux density (Table S5), producing efficiency ratios of 432:36:1 (UVB: UVA: PAR) for OCS and 402:32:1 for CS_2. These ratios aligned with previously reported ratios for methyl mercury photodemethylation efficiency (400:37:1),[50] underscoring the predominant role of UVB. Notably, UVB, accounting for less than 1% of solar radiation flux, contributed to nearly half of the photoproduction of OCS and CS_2 in the surface seawater, attributable to its higher energy. The potential increase in photoproduction in the upper ocean due to stratospheric ozone depletion and ocean stratification, consequences of global warming, merits attention.

3.3. Loss Processes of DMS, OCS, and CS_2. *3.3.1. Microbial Consumption and Photodegradation of DMS.* The average rates and rate constants (rate divided by concentration) of DMS microbial consumption in the surface seawater were 1.62 ± 0.69 nmol L^{-1} d^{-1} and 1.09 ± 0.22 d^{-1}, respectively. Consistent with production rates, high DMS consumption rates were predominantly observed in the KOE, with Station P1 recording the peak. A significant positive correlation was observed between the DMS microbial consumption rate and biological production rate (Figure S4), likely attributed to bacterial activities that mediate both processes, particularly robust in the nutrient-rich KOE. Overall, over half of the DMS produced was metabolized in situ by microorganisms (consumption-to-production rate ratio: 59.7% ± 8.4%), indicating a limited accumulation and consequently low DMS levels in the western North Pacific.

The rates for DMS photodegradation under natural light, UVB, UVA, and PAR at the sea surface were 1.50 ± 0.70, 0.70 ± 0.30, 0.61 ± 0.31, and 0.19 ± 0.17 nmol L^{-1} d^{-1}, respectively, with corresponding rate constants of 1.01 ± 0.23, 0.48 ± 0.15, 0.41 ± 0.12, and 0.12 ± 0.08 d^{-1}. UV radiation emerged as the predominant factor (>80%; Figure 2d) driving surface DMS photodegradation, aligning with previous research.[14,15] DMS photodegradation, primarily facilitated by secondary photosensitizers such as CDOM and nitrate,[51,52] occurs more rapidly in high-latitude regions abundant in photosensitizers and low-latitude regions with intense solar radiation (e.g., Station P27), as evidenced by the rate constants (Table S2). Upon normalization to photon flux density, the KOE displayed the

https://doi.org/10.1021/acs.est.3c07498
Environ. Sci. Technol. 2024, 58, 3235−3245

highest DMS photodegradation rate (Table S5), with UVB showing a significantly higher influence (UVB:UVA:PAR ratio of 463:39:1).

3.3.2. Hydrolysis of OCS and Chemical Removal of CS_2. Tables S3 and S4 presented the hydrolysis rates of OCS and chemical removal rates of CS_2 in surface seawater as 0.137 ± 0.040 and 3.83 × 10^{-3} ± 1.53 × 10^{-3} nmol L^{-1} d^{-1}, with corresponding rate constants of 3.16 ± 1.59 and 1.39 × 10^{-1} ± 8.69 × 10^{-2} d^{-1}, respectively. These rates, especially rate constants, exhibited an increasing trend from the north to south. According to the parametrized formula (Section 2.2.1), it is clear that this phenomenon was attributed to the temperature dependency of OCS hydrolysis, as KOE and NPSG seawater exhibited similar salinity and pH. The removal mechanism of CS_2 in seawater remains inadequately quantified and understood. Given CS_2's toxicity to fungi and bacteria,[53] it is commonly presumed to lack a biological removal pathway in marine environments. While CS_2 can undergo hydrolysis and oxidation through hydrogen peroxide,[22] the process is significantly slower than the sea-air exchange, implying the presence of alternate chemical pathways for CS_2 removal in seawater. Past research hypothesized a chemical sink with an approximate 10-day lifespan to explain Atlantic transect concentrations,[23] a concept corroborated by our rate constant measurements for CS_2 chemical removal. Furthermore, while our research did not identify specific additional pathways for CS_2 removal, we asserted that the seawater temperature plays a vital role in this process. In our study, the seawater temperature can explain 72.3% of variation of the CS_2 chemical removal rate constant (Figure S4), indicating that the CS_2 removal may be promoted by increasing seawater temperature with decreasing latitude. Scott's study also found that temperature increase significantly promoted the elimination of CS_2 by hydroxide based on laboratory simulations.[22]

3.3.3. Sea-Air Exchange of DMS, OCS, and CS_2. Sea-air fluxes of DMS, OCS, and CS_2 (Table S1) were 4.26 ± 2.10, 0.098 ± 0.062, and 0.077 ± 0.044 μmol m^{-2} d^{-1}, respectively, generally compared well with the previous findings in the western Pacific[28] and supported the climatological mean fluxes.[12,37] The western North Pacific was a net source of atmospheric DMS, OCS, and CS_2. Despite the higher seawater concentrations of these sulfides in the KOE, only the sea-air fluxes of OCS and CS_2 were higher in the KOE, and among them, only the sea-air flux of OCS exhibited statistical differences between the two regions (Figure 1c). This phenomenon may be attributed to the influence of wind speed and seawater temperature on the sea-air exchange process. A sensitivity analysis was conducted to assess the extent of influence exerted by various factors (seawater concentrations, temperature, and wind speed) on the sea-air fluxes (Figure S5). The results indicated that elevated concentrations, higher temperatures, and increased wind speeds all enhance sea-air exchange. The fluxes' response to these factors showed that, within the parameter variation range in the surveyed area, wind speed had the most substantial impact, followed by seawater gas concentrations. Additionally, significant correlations were observed exclusively between wind speed and sea-air flux (Figure S4), with wind speed accounting for 87.0%, 33.1%, and 50.5% of the variations in DMS, OCS, and CS_2 fluxes, respectively. Consequently, the elevated temperature in the NPSG stimulated the sea-air exchange to a certain degree. Additionally, it should be noted that the higher wind speed in the NPSG (7.6 m s^{-1} vs 6.5 m s^{-1} in the KOE, despite the lack of statistical significance) also promoted this process. Seawater DMS concentration increased to a lesser extent in the KOE region compared to OCS and CS_2, which is insufficient to offset the effects of temperature and wind speed, resulting in comparable sea-air fluxes between the two regions.

The higher sea-air fluxes of OCS and CS_2 may contribute to the higher atmospheric concentrations of OCS and CS_2 in the KOE compared to the NPSG. However, similar sea-air fluxes of DMS between the KOE and NPSG cannot explain the high atmospheric DMS level observed in the KOE. In addition to local emissions, based on the 72 h backward trajectories (Figure S6), air masses over the NPSG mainly originated from the surrounding ocean, suggesting oceanic emissions as the primary source of atmospheric DMS, OCS, and CS_2 in the region. In contrast, air masses over the KOE were significantly affected by northeastern China and Japan. Terrestrial air mass inputs may also increase the atmospheric concentrations of these sulfides in the KOE.[3] Besides, the rapid oxidation of DMS and CS_2 to methanesulfonic acid/sulfate and OCS in the atmosphere, which is accelerated by increasing temperature, could lead to their swift removal, resulting in lower atmospheric DMS and CS_2 concentrations in the NPSG compared with the KOE.

3.4. Fate of DMS, OCS, and CS_2 in the Mixed Layer. *3.4.1. Modeled Photochemical Processes Throughout the Mixed Layer.* The fate of marine DMS, OCS, and CS_2 depends on various source and sink processes. Assuming homogeneity in seawater properties within the mixed layer, rates derived from surface seawater measurements are generally applicable throughout this layer. However, radiation intensity variations in the mixed layer will affect the photochemical production and degradation processes. To extend experimental findings to the deep-water column, simulations of photodegradation of DMS and photoproduction of OCS and CS_2 were conducted throughout the entire upper ocean. Only the modeled results within the mixed layer are reliable; simulations below this layer offer merely a rough estimate of the photochemical rate trends in the euphotic zone.

Figure S7 displays vertical profiles of rates of DMS photodegradation and OCS and CS_2 photoproduction. Photochemical processes declined rapidly with an increasing depth. Although abundant organic matter facilitated photoreactions, it also accelerated the decay of these reactions in KOE seawater compared to NPSG. Each radiation waveband exhibited a unique variation trend in its photochemical rate profile, attributed to varying attenuation coefficients. In the top 10−30 m, UV radiation, particularly UVA over UVB, dominated photochemical reactions at most stations. With increasing depth, PAR gained prominence due to UV radiation's higher attenuation. Beyond the mixed layer, PAR emerged as the primary driver of photochemical processes at most stations owing to its superior penetration. The average photoreaction rate of the mixed layer was defined as the ratio of the vertically integrated rate across the mixed layer to its depth. Table S6 showed that within the mixed layer, UVB, UVA, and PAR accounted for 20.9% ± 6.3%, 50.5% ± 12.3%, 28.6% ± 17.4% for DMS photodegradation, 19.0% ± 3.8%, 48.2% ± 9.7%, 32.9% ± 10.9% for OCS photoproduction, and 20.0% ± 4.3%, 45.1% ± 7.1%, 35.0% ± 9.4% for CS_2 photoproduction, respectively, varying significantly from ratios observed at the sea surface. Across the entire mixed layer, UVA and PAR were the primary contributors to photochemical processes, with UVB playing a reduced role compared with the sea surface. Short-wavelength UVB, despite its higher energy, rapidly attenuated in seawater,

https://doi.org/10.1021/acs.est.3c07498
Environ. Sci. Technol. 2024, 58, 3235−3245

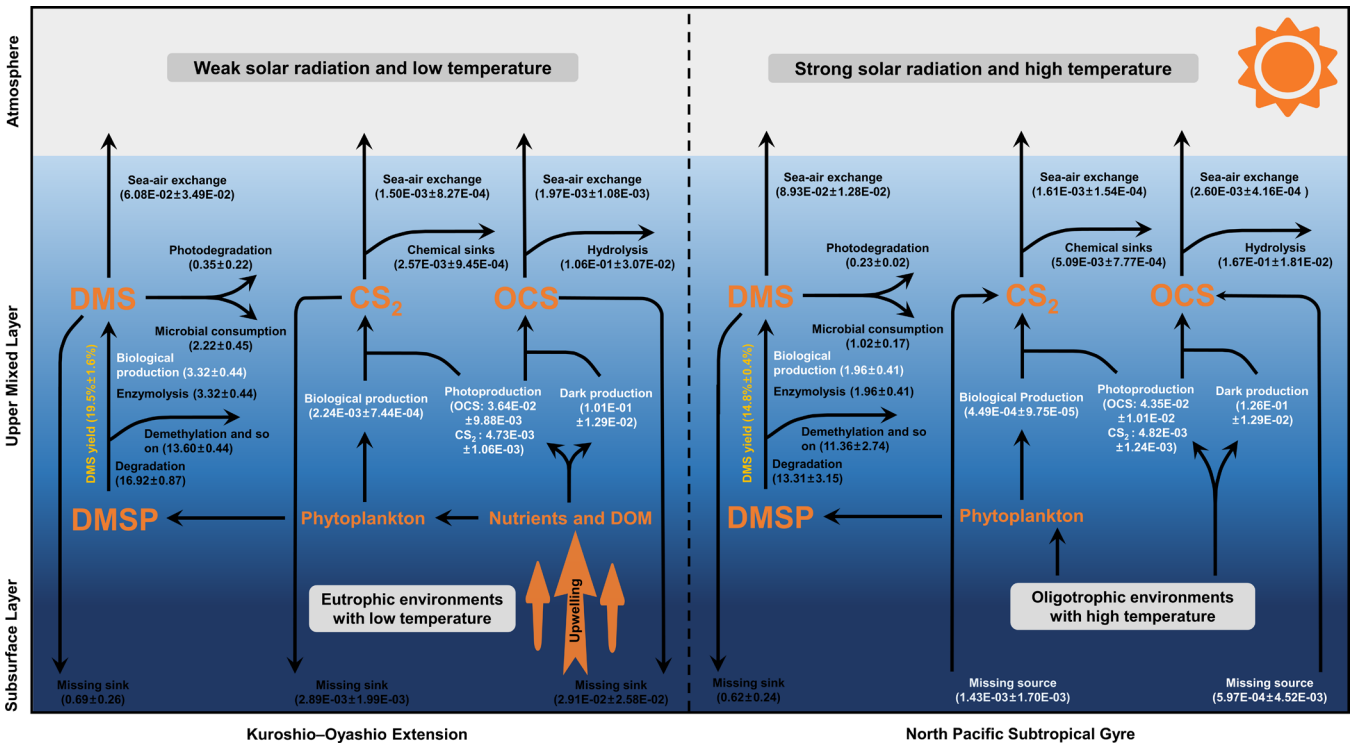

Figure 3. Source-sink budget models for the DMS, OCS, and CS_2 within the mixed layer in the KOE and NPSG regions of the western North Pacific. The numerical values in the figure indicate the mean rates (standard deviation) of sources and sinks within the mixed layer in the corresponding survey area, expressed in nmol L^{-1} d^{-1}.

remaining active only in shallow surface seawater of approximately 10−20 m.

3.4.2. Budgets of DMS, OCS, and CS_2 and Their Biogeochemical Controls. We developed a budget model (Figure 3), based on our research, to detail the source and loss processes of marine DMS, OCS, and CS_2 in the mixed layer. This model elucidated the biogeochemical processes governing the concentrations and fluxes of these sulfur gases. DMSP production by phytoplankton initiated the DMS cycle. Mesoscale eddies in the KOE-induced upwelling of nutrient-rich water, promoting phytoplankton growth and DMSP accumulation. Subsequently, stronger bacterial activity promoted DMSP degradation, and the nutrient-rich environment increased the proportion of DMSP cleavage to produce DMS. The resulting rapid biological production was responsible for the DMS accumulation in the KOE. The produced mixed-layer DMS will be removed through microbial consumption, photodegradation, and sea-air exchange. Abundant DMS and stronger bacterial activity also accelerated DMS microbial metabolism in the KOE, while the photodegradation was not significantly different between the regions. Despite higher seawater DMS concentration in the KOE, the lower temperatures and especially reduced wind speeds may hinder its outgassing to the atmosphere.

For the mixed layer budget, there was a discrepancy between sources and sinks of DMS, with a higher quantity of produced DMS than that removed (Table S2). Additionally, the DMSP biosynthesis by phytoplankton is a light-dependent process.[54,55] The incubation experiments under dark conditions can reduce the DMSP yield and thus may underestimate the biological production rate of DMS to some extent. This suggests that the actual difference between DMS sources and sinks could be more significant than that currently observed. Unidentified DMS sinks within the mixed layer, which have not been considered in this study, may contribute to this discrepancy. For example, a recent study identified the reaction of DMS with hypobromous acid as a potential marine DMS removal mechanism.[56] However, our study did not provide direct evidence of this pathway. Besides, we guess vertical mixing may serve as a potential sink of mixed-layer DMS. As indicated in Figure S8, a substantial gradient in DMS concentration between the mixed and subsurface layers could facilitate a considerable supplement of DMS to the latter. It cannot be ignored that the observed discrepancy may also partly result from uncertainties in the estimated rates of the production and removal processes. These uncertainties propagate, culminating in obvious ambiguity in the net difference between sources and sinks, as elucidated in Appendix S2 and Table S2. For the purposes of discussion, we tentatively attributed this unidentified sink entirely to vertical mixing, calculated as the discrepancy between the source and sink rates. Using the rates of each process, we quantitatively assessed their contribution to DMS removal in the mixed layer. Figure 2e illustrates that microbial consumption was the predominant DMS removal pathway, responsible for 59.7% ± 8.4% of the removal, while photodegradation accounted for only 10.9% ± 4.1% due to depth-related attenuation. Approximately 70% of DMS cycle occurred within the mixed layer, with sea-air exchange and vertical exchange transferring 3.2% ± 1.6% and 26.1% ± 9.9% of DMS, respectively, to the atmosphere and deeper ocean.

Plentiful photosensitizers (i.e., dissolved organic matter and nitrate)[16,49] and intense solar radiation were beneficial to the photoproduction of OCS/CS_2 in the KOE and NPSG, respectively. Abundant organic matter and a higher seawater temperature expedited the dark production of OCS in the KOE and NPSG, respectively. Notably, the KOE exhibited a relatively

https://doi.org/10.1021/acs.est.3c07498
Environ. Sci. Technol. 2024, 58, 3235−3245

rapid biological production of CS_2, in stark contrast to the negligible biological production in the nutrient-poor NPSG. But overall, the biological production rate of CS_2 was substantially lower than its photoproduction rate. When considering both photochemical and dark/biological production processes in the mixed layer, the overall production rates of CS_2 in the KOE and NPSG did not significantly differ (t test, $P > 0.05$). Interestingly, the total production rate of the OCS in the KOE was lower than that in the NPSG. These findings suggested that production processes may not be the key factor influencing the varying concentrations of OCS and CS_2 in these regions. Instead, removal mechanisms, such as hydrolysis and oxidation—processes that were accelerated by higher seawater temperatures—likely contributed to the lower gas concentrations observed in the NPSG.

Similarly, as presented in Tables S3 and S4, the production rates of OCS and CS_2 within the mixed layer generally exceeded their removal rates, a trend particularly pronounced in the KOE. For CS_2, the NPSG displayed a unique pattern, where its production rate was lower than the removal rate. Analyzing the concentration profiles of OCS and CS_2 at representative stations in the KOE and NPSG (Figure S8), we believed that vertical mixing may indeed play a nonnegligible role, despite the presence of unidentified sinks and measurement uncertainties. Specifically, in the NPSG (e.g., Station P27), the similar concentrations of OCS and CS_2 in the mixed and subsurface layers—attributable to the higher seawater temperature limiting accumulation in the mixed layer—resulted in a less pronounced vertical concentration gradient. This scenario possibly even led to gas transport from the subsurface to the mixed layer. We also quantified the vertical exchange rate as the difference between the source and sink rates. The relative contributions of each pathway to the source/sink of OCS and CS_2 in the mixed layer were presented in Figure 2f,g. Note that the role of vertical mixing switched between the source and sink for mixed-layer OCS and CS_2 in the survey area. For OCS production, dark reactions predominated, contributing 73.4% ± 7.1%, as photoreactions diminished with depth, contributing only 26.0% ± 6.7%. The impact of sea-air exchange on OCS was minimal, contributing just 1.5% ± 0.7% to its removal, due to a low concentration gradient between the ocean and atmosphere. Notably, most of the OCS (87.1% ± 17.8%) was directly removed in situ by hydrolysis in seawater, and this proportion gradually increased from north to south with rising temperatures. This trend correspondingly resulted in a gradual reduction in the percentage of downward vertical exchange from north to south. At the southernmost Station P27, the lower OCS concentration in the mixed layer even led to upward replenishment from the subsurface layer. In the case of CS_2, photoreactions, contributing 71.1% ± 14.9%, were the primary production mechanism, with their significance growing from north to south alongside a decrease in primary productivity. Biological production accounted for only 19.2% ± 12.5% of total sources. Outgassing (23.1% ± 7.0%) played an important role in CS_2 removal. Over half of CS_2 (59.1% ± 22.8%) was removed by hydrolysis, oxidation, and so on, and the contribution of these temperature-controlled chemical removal processes increased as latitude decreased. These variations in the intensity of chemical sinks altered the CS_2 concentration gradient between the mixed layer and deep ocean, thereby influencing the direction of vertical exchange: it acted as a sink in the mixed layer in the KOE, whereas in the NPSG, the situation was reversed.

Our study constrained the sources and sinks of marine volatile sulfides and provided the first comprehensive description of their mixed-layer cycle and budget. These field survey results and findings can be utilized as inputs or references for refining box models, which may have neglected certain processes such as the biological production of CS_2 and vertical exchange between the mixed and subsurface layers.[37] The improved model may contribute to reducing the uncertainty of marine sulfur emissions and identifying the missing source of atmospheric OCS.

■ ASSOCIATED CONTENT

Supporting Information

The Supporting Information is available free of charge at https://pubs.acs.org/doi/10.1021/acs.est.3c07498.

Sampling, analysis, and calculation; statistics and uncertainty analysis; oceanographic features of the western North Pacific; additional figures and tables (PDF)

■ AUTHOR INFORMATION

Corresponding Authors

Hong-Hai Zhang − *Frontiers Science Center for Deep Ocean Multispheres and Earth System, Key Laboratory of Marine Chemistry Theory and Technology, Ministry of Education, and College of Chemistry and Chemical Engineering, Ocean University of China, Qingdao 266100, China;* orcid.org/0000-0001-9576-4035; Email: honghaizhang@ouc.edu.cn

Gui-Peng Yang − *Frontiers Science Center for Deep Ocean Multispheres and Earth System, Key Laboratory of Marine Chemistry Theory and Technology, Ministry of Education, and College of Chemistry and Chemical Engineering, Ocean University of China, Qingdao 266100, China; Laboratory for Marine Ecology and Environmental Science, Laoshan Laboratory, Qingdao 266237, China;* orcid.org/0000-0002-0107-4568; Email: gpyang@mail.ouc.edu.cn

Authors

Feng Xu − *Frontiers Science Center for Deep Ocean Multispheres and Earth System, Key Laboratory of Marine Chemistry Theory and Technology, Ministry of Education, and College of Chemistry and Chemical Engineering, Ocean University of China, Qingdao 266100, China; Laboratory for Marine Ecology and Environmental Science, Laoshan Laboratory, Qingdao 266237, China*

Xiao-Song Zhong − *Frontiers Science Center for Deep Ocean Multispheres and Earth System, Key Laboratory of Marine Chemistry Theory and Technology, Ministry of Education, and College of Chemistry and Chemical Engineering, Ocean University of China, Qingdao 266100, China*

Shi-Bo Yan − *Frontiers Science Center for Deep Ocean Multispheres and Earth System, Key Laboratory of Marine Chemistry Theory and Technology, Ministry of Education, and College of Chemistry and Chemical Engineering, Ocean University of China, Qingdao 266100, China*

Jia-Wei Zhang − *Eco-Environmental Monitoring and Research Center, Pearl River Valley and South China Sea Ecology and Environment Administration, Ministry of Ecology and Environment, Guangzhou 510610, China*

Xin Ma − *Key Laboratory of Physical Oceanography, Ministry of Education, Ocean University of China, Qingdao 266100, China*

https://doi.org/10.1021/acs.est.3c07498
Environ. Sci. Technol. 2024, 58, 3235−3245

Zhao-Hui Chen − *Key Laboratory of Physical Oceanography, Ministry of Education, Ocean University of China, Qingdao 266100, China*

Complete contact information is available at: https://pubs.acs.org/10.1021/acs.est.3c07498

Notes

The authors declare no competing financial interest.

■ ACKNOWLEDGMENTS

We would like to thank the crew and captain of the R/V *"Dong Fang Hong 3"* for their support and cooperation throughout the investigation. We are also appreciative of the constructive comments of editors and three reviewers earnestly. This work was financially supported by the National Natural Science Foundation of China (grant numbers 42276042, 41976038, 41876082, and 42225601), the Laoshan Laboratory (grant numbers LSKJ202201701 and LSKJ202202904), and the Fundamental Research Funds for the Central Universities (grant numbers 202372001 and 202072001).

■ REFERENCES

(1) Turco, R. P.; Whitten, R. C.; Toon, O. B.; Pollack, J. B.; Hamill, P. OCS, Stratospheric Aerosols and Climate. *Nature* **1980**, *283* (5744), 283−285.

(2) Charlson, R. J.; Lovelock, J. E.; Andreae, M. O.; Warren, S. G. Oceanic Phytoplankton, Atmospheric Sulphur Cloud Albedo and Climate. *Nature* **1987**, *326* (6114), 655−661.

(3) Lee, C.-L.; Brimblecombe, P. Anthropogenic Contributions to Global Carbonyl Sulfide, Carbon Disulfide and Organosulfides Fluxes. *Earth-Science Rev.* **2016**, *160*, 1−18.

(4) Chang, R. Y.-W.; Sjostedt, S. J.; Pierce, J. R.; Papakyriakou, T. N.; Scarratt, M. G.; Michaud, S.; Levasseur, M.; Leaitch, W. R.; Abbatt, J. P. D. Relating Atmospheric and Oceanic DMS Levels to Particle Nucleation Events in the Canadian Arctic. *J. Geophys. Res.* **2011**, *116* (D17), D00S03.

(5) Ghahremaninezhad, R.; Norman, A.-L.; Abbatt, J.; Levasseur, M.; Thomas, J. L. Biogenic, Anthropogenic and Sea Salt Sulfate Size-Segregated Aerosols in the Arctic Summer. *Atmos. Chem. Phys.* **2016**, *16*, 5191−5202.

(6) Yan, J.; Jung, J.; Zhang, M.; Xu, S.; Lin, Q.; Zhao, S.; Chen, L. Significant Underestimation of Gaseous Methanesulfonic Acid (MSA) over Southern Ocean. *Environ. Sci. Technol.* **2019**, *53* (22), 13064−13070.

(7) Quinn, P. K.; Bates, T. S. The Case against Climate Regulation via Oceanic Phytoplankton Sulphur Emissions. *Nature* **2011**, *480* (7375), 51−56.

(8) Clarke, A. D.; Freitag, S.; Simpson, R. M. C.; Hudson, J. G.; Howell, S. G.; Brekhovskikh, V. L.; Campos, T.; Kapustin, V. N.; Zhou, J. Free Troposphere as a Major Source of CCN for the Equatorial Pacific Boundary Layer: Long-Range Transport and Teleconnections. *Atmos. Chem. Phys.* **2013**, *13* (15), 7511−7529.

(9) Lennartz, S. T.; Marandino, C. A.; Von hobe, M.; Andreae, M. O.; Aranami, K.; Atlas, E.; Berkelhammer, M.; Bingemer, H.; Booge, D.; Cutter, G.; Cortes, P.; Kremser, S.; Law, C. S.; Marriner, A.; Simó, R.; Quack, B.; Uher, G.; Xie, H.; Xu, X. Marine Carbonyl Sulfide (OCS) and Carbon Disulfide (CS_2): A Compilation of Measurements in Seawater and the Marine Boundary Layer. *Earth Syst. Sci. Data* **2020**, *12* (1), 591−609.

(10) Brühl, C.; Lelieveld, J.; Crutzen, P. J.; Tost, H. The Role of Carbonyl Sulphide as a Source of Stratospheric Sulphate Aerosol and Its Impact on Climate. *Atmos. Chem. Phys.* **2012**, *12* (3), 1239−1253.

(11) Chin, M.; Davis, D. D. Global Sources and Sinks of OCS and CS 2 and Their Distributions. *Global Biogeochem. Cycles* **1993**, *7* (2), 321−337.

(12) Hulswar, S.; Simó, R.; Galí, M.; Bell, T. G.; Lana, A.; Inamdar, S.; Halloran, P. R.; Manville, G.; Mahajan, A. S. Third Revision of the Global Surface Seawater Dimethyl Sulfide Climatology (DMS-Rev3). *Earth Syst. Sci. Data* **2022**, *14* (7), 2963−2987.

(13) Kremser, S.; Thomason, L. W.; Von hobe, M.; Hermann, M.; Deshler, T.; Timmreck, C.; Toohey, M.; Stenke, A.; Schwarz, J. P.; Weigel, R.; Fueglistaler, S.; Prata, F. J.; Vernier, J.-P.; Schlager, H.; Barnes, J. E.; Antuña-marrero, J.-C.; Fairlie, D.; Palm, M.; Mahieu, E.; Notholt, J.; Rex, M.; Bingen, C.; Vanhellemont, F.; Bourassa, A.; Plane, J. M. C.; Klocke, D.; Carn, S. A.; Clarisse, L.; Trickl, T.; Neely, R.; James, A. D.; Rieger, L.; Wilson, J. C.; Meland, B. Stratospheric Aerosol-Observations, Processes, and Impact on Climate. *Rev. Geophys.* **2016**, *54* (2), 278−335.

(14) Xu, F.; Yan, S.; Zhang, H.; Wu, Y.; Ma, Q.; Song, Y.; Zhuang, G.; Yang, G. Occurrence and Cycle of Dimethyl Sulfide in the Western Pacific Ocean. *Limnol. Oceanogr.* **2021**, *66* (7), 2868−2884.

(15) Ma, Q.; Zhang, H.; Xu, F.; Yang, G. Transformation Processes of Biogenic Dimethylated Sulfur Compounds in the Northwestern Pacific Continental Sea. *Limnol. Oceanogr.* **2022**, *67* (4), 903−917.

(16) Lennartz, S. T.; Von hobe, M.; Booge, D.; Bittig, H. C.; Fischer, T.; Gonçalves-araujo, R.; Ksionzek, K. B.; Koch, B. P.; Bracher, A.; Röttgers, R.; Quack, B.; Marandino, C. A. The Influence of Dissolved Organic Matter on the Marine Production of Carbonyl Sulfide (OCS) and Carbon Disulfide (CS_2) in the Peruvian Upwelling. *Ocean Sci.* **2019**, *15* (4), 1071−1090.

(17) Modiri gharehveran, M.; Shah, A. D. Indirect Photochemical Formation of Carbonyl Sulfide and Carbon Disulfide in Natural Waters: Role of Organic Sulfur Precursors, Water Quality Constituents, and Temperature. *Environ. Sci. Technol.* **2018**, *52* (16), 9108−9117.

(18) Ossola, R.; Tolu, J.; Clerc, B.; Erickson, P. R.; Winkel, L. H. E.; Mcneill, K. Photochemical Production of Sulfate and Methanesulfonic Acid from Dissolved Organic Sulfur. *Environ. Sci. Technol.* **2019**, *53* (22), 13191−13200.

(19) Pos, W. H.; Riemer, D. D.; Zika, R. G. Carbonyl Sulfide (OCS) and Carbon Monoxide (CO) in Natural Waters: Evidence of a Coupled Production Pathway. *Mar. Chem.* **1998**, *62* (1−2), 89−101.

(20) Kremser, S.; Jones, N. B.; Palm, M.; Lejeune, B.; Wang, Y.; Smale, D.; Deutscher, N. M. Positive Trends in Southern Hemisphere Carbonyl Sulfide. *Geophys. Res. Lett.* **2015**, *42* (21), 9473−9480.

(21) Xie, H.; Scarratt, M. G.; Moore, R. M. Carbon Disulphide Production in Laboratory Cultures of Marine Phytoplankton. *Atmos. Environ.* **1999**, *33* (21), 3445−3453.

(22) Elliott, S. Effect of Hydrogen Peroxide on the Alkaline Hydrolysis of Carbon Disulfide. *Environ. Sci. Technol.* **1990**, *24* (2), 264−267.

(23) Kettle, A. J. *Extrapolations of the Flux of Dimethylsulfide, Carbon Monoxide, Carbonyl Sulfide, and Carbon Disulfide from the Oceans*; York University, 2000.

(24) Tsunogai, S. The Western North Pacific Playing a Key Role in Global Biogeochemical Fluxes. *J. Oceanogr.* **2002**, *58* (2), 245−257.

(25) Tozuka, T.; Cronin, M. F.; Tomita, H. Surface Frontogenesis by Surface Heat Fluxes in the Upstream Kuroshio Extension Region. *Sci. Rep.* **2017**, *7* (1), 10258.

(26) Itoh, S.; Yasuda, I. Characteristics of Mesoscale Eddies in the Kuroshio−Oyashio Extension Region Detected from the Distribution of the Sea Surface Height Anomaly. *J. Phys. Oceanogr.* **2010**, *40* (5), 1018−1034.

(27) Uchiyama, Y.; Suzue, Y.; Yamazaki, H. Eddy-Driven Nutrient Transport and Associated Upper-Ocean Primary Production along the Kuroshio. *J. Geophys. Res. Ocean.* **2017**, *122* (6), 5046−5062.

(28) Xu, F.; Zhang, H.; Yan, S.; Sun, M.; Wu, J.; Yang, G.-P. Biogeochemical Controls on Climatically Active Gases and Atmospheric Sulfate Aerosols in the Western Pacific. *Environ. Res.* **2022**, *2023* (220), No. 115211. December

(29) Glatthor, N.; Höpfner, M.; Baker, I. T.; Berry, J.; Campbell, J. E.; Kawa, S. R.; Krysztofiak, G.; Leyser, A.; Sinnhuber, B.-M.; Stiller, G. P.; Stinecipher, J.; Von clarmann, T. Tropical Sources and Sinks of Carbonyl Sulfide Observed from Space. *Geophys. Res. Lett.* **2015**, *42* (22), 10082−10090.

(30) Kuai, L.; Worden, J. R.; Campbell, J. E.; Kulawik, S. S.; Li, K.-F. K.; Lee, M.; Weidner, R. J.; Montzka, S. A.; Moore, F. L.; Berry, J. A.; Baker, I.; Denning, A. S.; Bian, H.; Bowman, K. W.; Liu, J.; Yung, Y. L. Estimate of Carbonyl Sulfide Tropical Oceanic Surface Fluxes Using Aura Tropospheric Emission Spectrometer Observations. *J. Geophys. Res. Atmos.* **2015**, *120*, 20. 11,11−12,23

(31) Whelan, M. E.; Lennartz, S. T.; Gimeno, T. E.; Wehr, R.; Wohlfahrt, G.; Wang, Y.; Kooijmans, L. M. J. J.; Hilton, T. W.; Belviso, S.; Peylin, P.; Commane, R.; Sun, W.; Chen, H.; Kuai, L.; Mammarella, I.; Maseyk, K.; Berkelhammer, M.; Li, K.-F.; Yakir, D.; Zumkehr, A.; Katayama, Y.; Ogée, J.; Spielmann, F. M.; Kitz, F.; Rastogi, B.; Kesselmeier, J.; Marshall, J.; Erkkilä, K.-M.; Wingate, L.; Meredith, L. K.; He, W.; Bunk, R.; Launois, T.; Vesala, T.; Schmidt, J. A.; Fichot, C. G.; Seibt, U.; Saleska, S.; Saltzman, E. S.; Montzka, S. A.; Berry, J. A.; Campbell, J. E. Reviews and Syntheses: Carbonyl Sulfide as a Multi-Scale Tracer for Carbon and Water Cycles. *Biogeosciences* **2018**, *15* (12), 3625−3657.

(32) Wanninkhof, R. Relationship between Wind Speed and Gas Exchange over the Ocean Revisited. *Limnol. Oceanogr. Methods* **2014**, *12* (6), 351−362.

(33) Wolfe, G. V.; Kiene, R. P. Radioisotope and Chemical Inhibitor Measurements of Dimethyl Sulfide Consumption Rates and Kinetics in Estuarine Waters. *Mar. Ecol.: Prog. Ser.* **1993**, *99* (3), 261−269.

(34) Kiene, R.; Gerard, G. Evaluation of Glycine Betaine as an Inhibitor of Dissolved Dimethylsulfoniopropionate Degradation in Coastal Waters. *Mar. Ecol.: Prog. Ser.* **1995**, *128* (1−3), 121−131.

(35) Simó, R.; Pedrós-alió, C.; Malin, G.; Grimalt, J. O. Biological Turnover of DMS, DMSP and DMSO in Contrasting Open-Sea Waters. *Mar. Ecol.: Prog. Ser.* **2000**, *203*, 1−11.

(36) Elliott, S.; Lu, E.; Rowland, F. S. Rates and Mechanisms for the Hydrolysis of Carbonyl Sulfide in Natural Waters. *Environ. Sci. Technol.* **1989**, *23* (4), 458−461.

(37) Lennartz, S. T.; Gauss, M.; Von hobe, M.; Marandino, C. A. Monthly Resolved Modelled Oceanic Emissions of Carbonyl Sulphide and Carbon Disulphide for the Period 2000−2019. *Earth Syst. Sci. Data* **2021**, *13* (5), 2095−2110.

(38) Kloster, S.; Feichter, J.; Maier-reimer, E.; Six, K. D.; Stier, P.; Wetzel, P. DMS Cycle in the Marine Ocean-Atmosphere System-a Global Model Study. *Biogeosciences* **2006**, *3* (1), 29−51.

(39) De boyer montégut, C. Mixed Layer Depth over the Global Ocean: An Examination of Profile Data and a Profile-Based Climatology. *J. Geophys. Res.* **2004**, *109* (C12), C12003.

(40) Vila-costa, M.; Del valle, D. A.; González, J. M.; Slezak, D.; Kiene, R. P.; Sánchez, O.; Simó, R. Phylogenetic Identification and Metabolism of Marine Dimethylsulfide-Consuming Bacteria. *Environ. Microbiol.* **2006**, *8* (12), 2189−2200.

(41) Vila-costa, M.; Kiene, R. P.; Simí, R. Seasonal Variability of the Dynamics of Dimethylated Sulfur Compounds in a Coastal Northwest Mediterranean Site. *Limnol. Oceanogr.* **2008**, *53* (1), 198−211.

(42) Simó, R. Production of Atmospheric Sulfur by Oceanic Plankton: Biogeochemical, Ecological and Evolutionary Links. *Trends Ecol. Evol.* **2001**, *16* (6), 287−294.

(43) Kiene, R. P.; Linn, L. J. The Fate of Dissolved Dimethylsulfoniopropionate (DMSP) in Seawater: Tracer Studies Using 35S-DMSP. *Geochim. Cosmochim. Acta* **2000**, *64* (16), 2797−2810.

(44) Cutter, G. A.; Cutter, L. S.; Filippino, K. C. Sources and Cycling of Carbonyl Sulfide in the Sargasso Sea. *Limnol. Oceanogr.* **2004**, *49* (2), 555−565.

(45) Radford-knęry, J.; Cutter, G. A. Biogeochemistry of Dissolved Hydrogen Sulfide Species and Carbonyl Sulfide in the Western North Atlantic Ocean. *Geochim. Cosmochim. Acta* **1994**, *58* (24), 5421−5431.

(46) Launois, T.; Belviso, S.; Bopp, L.; Fichot, C. G.; Peylin, P. A New Model for the Global Biogeochemical Cycle of Carbonyl Sulfide − Part 1: Assessment of Direct Marine Emissions with an Oceanic General Circulation and Biogeochemistry Model. *Atmos. Chem. Phys.* **2015**, *15* (5), 2295−2312.

(47) Von hobe, M.; Cutter, G. A.; Kettle, A. J.; Andreae, M. O. Dark Production: A Significant Source of Oceanic COS. *J. Geophys. Res. Ocean.* **2001**, *106* (C12), 31217−31226.

(48) Xie, H.; Moore, R. M.; Miller, W. L. Photochemical Production of Carbon Disulphide in Seawater. *J. Geophys. Res. Ocean.* **1998**, *103* (C3), 5635−5644.

(49) Li, J.-L.; Zhai, X.; Du, L. Effect of Nitrate on the Photochemical Production of Carbonyl Sulfide From Surface Seawater. *Geophys. Res. Lett.* **2022**, *49* (13), 1−8.

(50) Black, F. J.; Poulin, B. A.; Flegal, A. R. Factors Controlling the Abiotic Photo-Degradation of Monomethylmercury in Surface Waters. *Geochim. Cosmochim. Acta* **2012**, *84*, 492−507.

(51) Galí, M.; Kieber, D. J.; Romera-castillo, C.; Kinsey, J. D.; Devred, E.; Pérez, G. L.; Westby, G. R.; Marrasé, C.; Babin, M.; Levasseur, M.; Duarte, C. M.; Agustí, S.; Simó, R. CDOM Sources and Photobleaching Control Quantum Yields for Oceanic DMS Photolysis. *Environ. Sci. Technol.* **2016**, *50* (24), 13361−13370.

(52) Bouillon, R.-C.; Miller, W. L. Photodegradation of Dimethyl Sulfide (DMS) in Natural Waters: Laboratory Assessment of the Nitrate-Photolysis-Induced DMS Oxidation. *Environ. Sci. Technol.* **2005**, *39* (24), 9471−9477.

(53) Kiene, R. P. Microbial Cycling of Organosulfur Gases in Marine and Freshwater Environments. *Int. Vereinigung für Theor. und Angew. Limnol. Mitteilungen* **1996**, *25* (1), 137−151.

(54) Gali, M.; Ruiz-gonzàlez, C.; Lefort, T.; Gasol, J. M.; Cardelús, C.; Romera-castillo, C.; Simó, R. Spectral Irradiance Dependence of Sunlight Effects on Plankton Dimethylsulfide Production. *Limnol. Oceanogr.* **2013**, *58* (2), 489−504.

(55) Galí, M.; Saló, V.; Almeda, R.; Calbet, A.; Simó, R. Stimulation of Gross Dimethylsulfide (DMS) Production by Solar Radiation. *Geophys. Res. Lett.* **2011**, *38*, 15.

(56) Müller, E.; Von gunten, U.; Bouchet, S.; Droz, B.; Winkel, L. H. E. Reaction of DMS and HOBr as a Sink for Marine DMS and an Inhibitor of Bromoform Formation. *Environ. Sci. Technol.* **2021**, *55* (8), 5547−5558.

https://doi.org/10.1021/acs.est.3c07498
Environ. Sci. Technol. 2024, 58, 3235−3245